INTERNATIONAL JOURNAL FOR NUMERICAL METHODS IN FLUIDS
Int. J. Numer. Meth. Fluids 2004; **44**:115–133 (DOI: 10.1002/fld.617)

Resolution of the flow in clarifiers by using a stabilized finite element method

P. Vellando[1,*,†], J. Puertas[2] and I. Colominas[1]

[1]*Group of Numerical Methods in Engineering (GNME), ETS de Ingenieros de Caminos, Canales y Puertos, Universidad de La Coruña, Campus de Elviña, 15071 La Coruña, Spain*
[2]*Área de Ingeniería Hidráulica, Dpto. de Métodos Matemáticos y de Representación, ETS de Ingenieros de Caminos, Canales y Puertos, Universidad de La Coruña, Campus de Elviña, 15071 La Coruña, Spain*

SUMMARY

The description of the flow that takes place in clarifiers and other wastewater treatment basins may be a powerful tool to attain an optimum design of these structures, in order to make the most of the wastewater treatment plant resources. Some authors have attempted so by making use of the potential flow or the Stokes equations. When these simplifications are used, an approximation of the flow for slow creeping conditions is obtained, but only the resolution of the all-term-including Navier–Stokes equations will allow us to detect the real streamlines and the vortices that show up for even very slow water flows. The use of the Navier–Stokes formulae as the governing equations involves the appearance of complex stability problems that do not show up for the previously mentioned simplifications. In the present work a stable finite element method for the resolution of the Navier–Stokes equations is presented, verified, and used in the resolution of some wastewater treatment flow problems with very interesting results. Copyright © 2004 John Wiley & Sons, Ltd.

KEY WORDS: wastewater treatment; clarifiers; viscous incompressible flow; FEM; Navier–Stokes; SUPG

1. INTRODUCTION

A finite element formulation that solves the Navier–Stokes equations in a stable and efficient way has been released. Once this code has been evaluated, it has been used in the resolution of some practical engineering problems related to the wastewater industry. The obtaining of

*Correspondence to: P. Rodriguez-Vellando, ETS Ingenieros de Caminos, Canales y Puertos, Universidad de La Coruna, Campus de Elviña, 15071 La Coruna, Spain.
†E-mail: vellando@iccp.udc.es, http://caminos.udc.es/gmni

Contract/grant sponsor: Private company ENDESA
Contract/grant sponsor: European Union FEDER project
Contract/grant sponsor: Foundation of Civil Engineering of Galicia
Contract/grant sponsor: Ministry of Science and Technology
Contract/grant sponsor: Regional Government of Galicia

Received 18 November 2002
Revised 13 June 2003

the flow variables in these real cases may provide a powerful tool in order to allow for an improvement in the geometric features of the flow basins. Only through the comprehensive knowledge of the hydrodynamic variables, will the flow be not only evaluated but also fully understood. As a consequence, an adequate design of the basins and channels may be carried out, based upon an efficient and reliable numerical technique, resulting in great cost savings.

The finite element method is a numerical procedure for solving the differential equations that govern a wide variety of physical problems. The basis of this numerical technique are established in '*the finite element method*' written in 1967 by Zienkiewicz and Taylor [1]. This technique subdivides the domain of definition into a finite number of smaller regions, and uses the weighted residuals method so as to transform the governing differential equations into a set of discrete integral equations. This system of equations gives as a result, the value of the unknowns at the nodal points of the basic elements, being an approximation to the problem posed in the governing equations. The application of the finite element method to the flow problems requires some modifications with respect to the formulation used for the structural stress analysis problems, which were its first application. Some of these modifications have been borrowed from the finite difference or finite volume approaches, and many others have been specifically developed for finite elements. When applying the finite element analysis to the problems of the rigid body, the weighted residual method can be exclusively applied to the Newton's second law, which for statics clearly turns out to be the equilibrium equation. On the contrary, when dealing with fluids, the shape is not any more conserved, and apart from stating the equilibrium of momentum, we have to ensure for the continuity of mass. Consequently, we have two equations to be verified at the same time, and the finite element formulation should also account for the verification of both. The only set of unknowns in the conventional structural analysis is that of the displacements, as a consequence, the system obtained thanks to the application of the finite element method, gives the displacements in the structure depending on the stiffness matrix, and the load vector. In the flow problems, we are headed towards the so-called mixed finite element methods, in which both the velocity and pressure set of unknowns have to be treated simultaneously. Many different algorithms have been used trying to improve the numerical behaviour of these finite element formulations for fluids, which some authors [2, 3], agree to divide into velocity–pressure integrated, segregated and penalty methods. A 2D penalty formulation will be presented in this work for the resolution of the laminar viscous incompressible flow.

The use of a Galerkin formulation, that takes weighting functions equal to trial functions when solving the Navier–Stokes equations, may lead to some problems of instability in the obtaining of the flow by the finite element method. To avoid this difficulty, some so-called stabilization procedures have been released. The stiffness matrix resulting from structural problems solved by the finite element method is symmetric, instead the 'stiffness' matrix obtained for fluids is non-symmetric and the use of symmetric weighting functions may lead to some instability problems. The faster the flow turns, the more non-symmetric the coefficient matrix becomes. In practice this is featured by the appearance of some spurious node-to-node oscillations also known as 'wiggles'. One way of avoiding these oscillations is to carry out a refinement in the mesh, such that convection no longer dominates on an element level, but this refinement turns to be a memory resources sink. This point will be avoided in this work by the use of a stabilization technique of the SUPG type, for the algorithms considered in it.

The 2D Navier–Stokes equations assume a flow that takes place on a two-dimensional plane, and it is consequently laminar in that sense. The shallow water formulation has been

also considered in this work as a way of including the third dimension in the calculations that allows for an adequate treatment of the free surface. The shallow water formulation gives a meaningful solution for flows in which the depth is small compared to the horizontal dimension. The integration in depth of the 3D Navier–Stokes formulation causes the dependence of the continuity equation with respect to depth, and consequently the appearance of some quasi-non-linear terms that depend on both the velocity and the depth. These equations are solved thanks to a newly developed iterative algorithm, which will be solved based on a velocity-pressure integrated formulation. The integration in depth of the 3D Navier–Stokes equations allows for the empirical evaluation of the energy losses taking place in the flow on a Manning basis. The Manning formula evaluates empirically the overall energy losses taking place in the fluid flow, including those related with the turbulent effects. This formulation does not capture the turbulent eddies taking place within the fluid flow but takes into account the turbulent energy losses. Many numerical resolutions of the incompressible flow use the Manning approach to evaluate these turbulent effects. However, most of the available numerical models neglect the viscous effects compared to the turbulent ones and the viscous term is dropped from the equations. The present shallow water formulation incorporates a Manning term but does not get rid of the viscous term, allowing for the evaluation of the overall turbulent losses, together with the viscous effects.

A code will be written based upon these particulars, and will be also validated by its comparison with available numerical and empirical reference results. Once the program has been validated, it will be used in the resolution of some wastewater problems, and their results will be presented. Some authors have attempted to evaluate the flow in clarifiers by using the Stokes hypothesis, or in other words ignoring the convective term in the Navier–Stokes equations. The potential flow equations are also used by some authors to evaluate these flows. When these simplifications are used, an approximation of the behaviour of the flow is obtained, but a very important part of the flow features is lost.

Some flow problems related to sewage disposal will be solved by making use of our code, and their results will be commented upon. We will focus on the obtaining of the flow in some of the most commonly used clarification and flocculation basins. The evaluation of the pressure and velocity of the flow in these basins will provide useful information about the flow properties. The data about the streamlines and velocity field distribution will allow us to know where the main recirculation regions are taking place. This information will be priceless for the purpose of obtaining the geometrical parameters of the basins in order to achieve a better performance of the treatment plant. The obtaining of this optimum geometry will permit to avoid the appearance of the recirculation regions, modifying in this way the detention times within the basin. Thanks to the information obtained by this numerical evaluation of the flow, the water treatment basins and channels can consequently be designed to fit the requirements of the processes being carried out.

2. GOVERNING EQUATIONS

The relationships to be held are the dynamic and the continuity equations. The first one gives the variation in the momentum as the summation of the acting forces on the volume of integration. To this condition we should add a second one, which states that in the absence of sources and sinks, the total mass is conserved. Both equalities make up the Navier–Stokes

equations. Using the indicial notation, we can express the steady Navier–Stokes equations as

$$\begin{aligned} u_j u_{i,j} &= -\frac{1}{\rho} p_{,i} + \nu u_{i,jj} + f_i \\ u_{i,i} &= 0 \quad \text{in } \Omega \end{aligned} \tag{1}$$

together with the boundary conditions:

$$u_i]_{\Gamma_1} = b_i \quad \sigma_{ij} n_j]_{\Gamma_2} = t_i \tag{2}$$

where u_i is the velocity, p is the pressure, f_i is the body force per unit mass, ρ is density, ν is the cinematic viscosity, Γ_1 and Γ_2 are two non-overlapping subsets of the piecewise smooth domain boundary Γ, b_i is the velocity vector prescribed in Γ_1, t_i is the traction vector prescribed on Γ_2, σ_{ij} is the stress along the boundary Γ_2, and n_j is the outward unit vector normal to Γ_2.

The 2D or laminar Navier–Stokes equations do not take into account the third dimension in space, and provide with the velocities and pressures of a theoretical planar flow. Nevertheless, for many real flow problems, the third dimension in space is very important. The 3D Navier–Stokes algorithms involve very high computational costs; moreover they present a great difficulty in the treatment of the free surface. The shallow water equations are a simplification of the Navier–Stokes equations, which can be used when the main direction of the flow is the horizontal one and the distribution of the horizontal velocity along the vertical direction can be assumed as uniform. These equations assume that the vertical acceleration of the fluid is negligible and that a hydrostatic distribution of the pressure can be adopted. When a 2D Navier–Stokes equation is used, the continuity equation is only held on a 2D basis. Nevertheless, the shallow water equations allow for the verification of the continuity equation on a 3D sense, providing with adequate results for the depth field, even when important changes in the depth are taking place within the domain.

Integrating the steady 3D Navier–Stokes equations in depth, it is obtained:

$$\begin{aligned} h u_{i,i} + u_i h_{,i} &= 0 \\ u_j u_{i,j} &= -g h_{,i} + \nu u_{i,jj} + g\left(S_{0i} - \frac{n^2 u_i \sqrt{u_j^2}}{R_h^{4/3}}\right) \end{aligned} \tag{3}$$

together with the boundary conditions:

$$u_i]_{\Gamma_1} = b_i \quad h]_{\Gamma_2} = d \tag{4}$$

where h is the depth, g is the gravity force, S_{0i} is the geometric slopes, d is the depth prescribed on Γ_2, R_h is the hydraulic radius and n is the Manning coefficient.

3. FINITE ELEMENT FORMULATION

3.1. Penalty laminar formulation

One of the main difficulties found when obtaining a numerical solution for the Navier–Stokes equations is that apart from verifying the dynamic constitutive equation, the solutions must satisfy in addition the incompressibility condition. The mixed finite element formulations lead

to a system in which both velocity and pressure are taken as the unknowns [4]. So as to reduce the dimension of the resulting system of equations, a penalty formulation can also be used. The penalty formulation provides with the possibility of imposing the incompressibility constraint without solving an auxiliary pressure equation, by replacing the continuity equation with the expression:

$$u_{i,i} = -\varepsilon p \tag{5}$$

where the so-called penalty parameter ε is a number close to zero. This equation is incorporated into the dynamic equation, and therefore a system that depends on both velocity and pressure is transformed into a velocity-dependant single equation, that converges to the fully incompressible problem as ε approaches zero [5–7]. Once we have applied the weighted residuals method, the following integral dynamic equation is obtained:

$$\int_{\Omega_h} w_i^h (u_j^h u_{i,j}^h - f_i)\,\mathrm{d}\Omega + \nu \int_{\Omega_h} w_{i,j}^h u_{i,j}^h\,\mathrm{d}\Omega + \int_{\Omega_h} \frac{1}{\varepsilon} u_{i,i}^h w_{i,i}^h\,\mathrm{d}\Omega - \int_{\Gamma_2} t_i^h w_i^h\,\mathrm{d}\Gamma_2 + \sum_c \bar{p}_i^h \left(u_j^h u_{i,j}^h - \nu u_{i,jj}^h - \frac{1}{\varepsilon}(u_{i,i}^h)_{,i} - f_i \right) \mathrm{d}\Omega = 0 \tag{6}$$

where $\bar{w}_i = w_i + \bar{p}_i$ are the SUPG weighting functions to be specified later in the text and the h superscript stands for the discretization being carried out in our formulation, in terms of a structured mesh. Once the elementary matrices have been calculated they can be assembled to obtain the non-linear system:

$$\mathbf{C}_v(\mathbf{u},\mathbf{v})\underline{v} + \nu \mathbf{A}_v \underline{v} + \frac{1}{\varepsilon} \mathbf{B}_\varepsilon \underline{v} = \mathbf{f} \tag{7}$$

where $\mathbf{C}_v(\mathbf{u},\mathbf{v})$ is the convective matrix, $\mathbf{A}_v$ is the viscous matrix, $\mathbf{B}_\varepsilon$ is the penalty matrix, $\mathbf{u}$ is the velocity vector in the x direction, $\mathbf{v}$ is the velocity vector in the y direction, $\mathbf{f}$ is the external forces vector and $\underline{v}$ is the velocity vector. The non-linearities introduced in the system by the convective term $\mathbf{C}_v(\mathbf{u},\mathbf{v})\underline{v}$ are solved by using a successive approximation method, which can be mathematically expressed as

$$\int_{\Omega_h} \bar{w}_i u_j u_{i,j}\,\mathrm{d}\Omega \approx \int_{\Omega_h} \bar{w}_i u_j^{n-1} u_{i,j}^n\,\mathrm{d}\Omega \tag{8}$$

where the superscripts n and $n-1$ stand for the values of the variables in the present and previous iterations. This linearization technique has shown to provide with good results in the resolution of the Navier–Stokes equations [8].

Once the velocity field has been obtained, the pressure field can be calculated as a post-processing result, by using the formula:

$$p^h = -\frac{1}{\varepsilon} u_{i,i}^h \tag{7'}$$

The solution to Equation (6) will approximate that of the initial problem as ε tends to zero, provided that the penalty consistency condition is verified. If not, the use of the penalty formulation could lead to the obtaining of a non-singular coefficient matrix associated to the penalty term. As ε tends to zero, this term may dominate the system of equations, therefore the

whole problem could be over-constrained, and the only possible solution could be the trivial one [5]. This problem can be avoided by making a so-called *selective reduced integration* of the elementary matrices involved in the resolution of the problem. A reduced numerical integration consists in using a quadrature rule that is not exact for the polynomials considered. The use of a one point Gauss quadrature rule for the integration of the quadratic functions in the penalty term transforms the associated 'penalty' matrix into a rank deficient matrix, and consequently 'unlocks' the obtaining of a non-trivial solution [9].

3.2. *Shallow Water formulation*

For the resolution of the shallow water equations we will use here a finite element mixed approach in which the unknowns of the resulting system of equations will be both the velocity and the depth. If we apply the weighted residuals method on both the dynamic and continuity shallow water equations, we would obtain

$$\int_{\Omega_h} w_i^h (u_j^h u_{i,j}^h - g(S_{0i}^h - S_{fi}^h))\,\mathrm{d}\Omega + \nu \int_{\Omega_h} w_{i,j}^h u_{i,j}^h\,\mathrm{d}\Omega - g\int_{\Omega_h} w_{i,i}^h h^h\,\mathrm{d}\Omega - \int_{\Gamma_2^h} t_i^h w_i^h\,\mathrm{d}\Gamma_2$$

$$+\sum_e \int_{\Omega_e} \bar{p}_i^h (u_j^h u_{i,j}^h - \nu u_{i,jj}^h + g h_{,i}^h - g(S_{0i}^h - S_{fi}^h))\mathrm{d}\Omega = 0$$

$$\int_{\Omega_h} q^h (h^h u_{i,i}^h + u_i^h h_{,i}^h)\,\mathrm{d}\Omega - 0 \tag{8'}$$

Now we find products of both the velocity and the depth among the terms included in the dynamic equation. The existence of these terms, allows for the verification of the conservation of mass in a pseudo-3D basis, but introduces some pseudo-non-linearities in our formulation that have to be solved by employing another numerical approach [10]. When using a mixed formulation in the resolution of the Navier–Stokes equations one of the sources of instability is the one produced by an inappropriate combination of the interpolation functions for the velocity and pressure unknowns. An equal interpolation may provide good results for the velocity but a meaningless solution for the depths [11]. The Q1P0 basic pair (bilinear velocity-constant pressure) has shown to provide with stable solutions even not satisfying strictly the LBB condition and will be used in the calculations [12].

The linearization of the pseudo-non-linearities that appear in the continuity equation is going to be carried out on a finite differences basis. For the first iteration it will be assumed that the depth values in the continuity equation are equal to the outflow given depth. In the following iterations to be carried out in order to solve for the convection, the depths and gradients of depth in the continuity equation will be evaluated from the results of the former iteration, and this evaluation will be carried out in terms of a finite differences approach to obtain the star depths and star gradients of the depth. For details you can refer to Reference [12].

After each iteration for convection has been solved, the star depths and star gradients of the depth are calculated and re-fed into the continuity equation. The use of this algorithm developed by the authors in the resolution of the Shallow Water equations achieves very good numerical results as will be seen in the numerical examples. The general procedure

for the obtaining of the steady system of differential equations could be written in its matrix form as

$$\mathbf{C}_v(\mathbf{u},\mathbf{v})\underline{v} + \nu\mathbf{A}_v\underline{v} - \mathbf{B}\mathbf{h} - \mathbf{f} \tag{9}$$

$$\mathbf{D}(\mathbf{h}^*)\underline{v} + \mathbf{E}(\dot{\mathbf{h}}^*)\underline{v} = \mathbf{0} \tag{10}$$

where $\mathbf{C}_v(\mathbf{u},\mathbf{v})$ is the convective matrix, $\mathbf{A}_v$ is the viscous matrix, $\mathbf{B}$ is the depth matrix, $\mathbf{f}$ is external forces vector, $\mathbf{D}(\mathbf{h}^*)$ is the star depth matrix, $\mathbf{E}(\dot{\mathbf{h}}^*)$ is the star gradient of depth matrix, $\mathbf{f}$ is the external forces vector, $\mathbf{h}$ is the depth vector and $\underline{v}$ is the velocity vector.

3.3. *SUPG stabilization of the algorithms*

The SUPG (streamline/upwinding Petrov–Galerkin) technique, first developed by Brookes [13], succeeds in eliminating the spurious velocity field, without carrying out a severe refinement in the mesh, by considering weighting functions that differ from trial functions in an upwinding term. This method was first released for the transport equation, and its generalization to the Navier–Stokes equation brings an additional problem; that is the appearance of an excessive diffusion normal to the flow. The SUPG method eliminates this spurious crosswind diffusion by considering an artificial diffusion that acts only in the direction of the flow. The above formulations include a SUPG term in the dynamic weighting functions that are defined as follows:

$$\bar{w}_i = w_i + \bar{p}_i \quad \text{with} \quad \bar{p}_i^h = \frac{\bar{k}\hat{u}_j^h w_{i,j}^h}{\|\mathbf{u}^h\|} \tag{11}$$

where the multi-dimensional definition of the diffusion coefficient $\bar{k}$ is given by

$$\hat{u}_i = \frac{u_i}{\|\mathbf{u}\|}, \quad \|\mathbf{u}\|^2 = u_i u_i, \quad \bar{k} = \frac{\bar{\xi}u_\xi^h h_\xi + \bar{\eta}u_\eta^h h_\eta}{2} \tag{12}$$

where

$$\bar{\xi} = \left(\coth\alpha_\xi - \frac{1}{\alpha_\xi}\right), \quad \bar{\eta} = \left(\coth\alpha_\eta - \frac{1}{\alpha_\eta}\right)$$

$$\alpha_\xi = \frac{u_\xi^h h_\xi}{2\nu}, \quad \alpha_\eta = \frac{u_\eta^h h_\eta}{2\nu} \tag{13}$$

$$u_\xi^h = e_{\xi i}u_{ci}^h, \quad u_\eta^h = e_{\eta i}u_{ci}^h$$

where h_ξ, h_η and $e_{\xi i}, e_{\eta i}$ are the characteristic basic-element lengths and unit vectors in the direction of the local axes ξ and η (see Figure 1). The parameters α_ξ and α_η are the directional Reynolds numbers of the basic element, u_{ci}^h is the velocity in the interior of the element and ν is the kinematic viscosity of the fluid. Different versions of the streamline upwind formulation have been used by other authors and can be found in [3, 7, 14]. The present weighting functions will be used in the penalty laminar and in the shallow water formulation explained before.

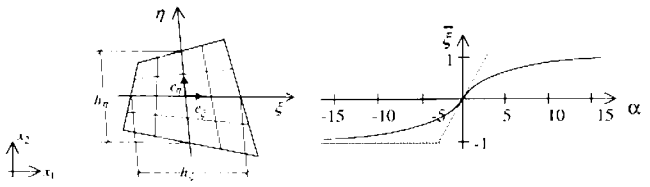

Figure 1. Characteristic basic-element lengths and unit vectors. Optimal rule for the approximation of $\bar{\xi}$ y $\bar{\eta}$.

4. NUMERICAL RESULTS

4.1. The Backward-facing step benchmark problem

The backward-facing step benchmark problem will be used for verification purposes. The backward step is based upon a simple geometry where flow separation and reattachment occur. Experimental data for this problem can be found in Armaly *et al.* [15], who also solved this problem numerically by using a control-volume-based finite difference method.

The geometry and boundary conditions considered for this benchmark problem have been those used in Reference [15]. An expansion ratio of 1:1.94 has been considered for the widening of the channel, which has a total length of 50 so as to allow for the vortices to take place. The inlet boundary has been located at 3.5 step heights upstream of the expansion corner. The domain has been split into 2850 Q1P0 basic non-regular elements with 3021 nodes. The mesh is coarser at the outlet and more refined at the left-hand side of the channel, so as to allow for a better accuracy in the regions where the primary vortices occur. A bias parameter of 0.5 has been used for this purpose along the x-axis, therefore the width of the basic elements at the inlet is one half of that of the elements at the outlet, and the height of the basic elements is uniform within the whole domain. The mesh can be seen in Figure 2, where a magnifying factor of two has been used for the y-axis. A parabolic horizontal velocity profile has been imposed at the inlet with a maximum velocity of 1, and the velocity is equal to zero at the boundaries. The lateral sides have been considered as solid boundaries and the no-slip condition has been imposed on them. Finally, a zero traction condition has been imposed at the outlet.

The flow has been obtained for a Reynolds number between 100 and 1200. The Reynolds number has been defined as $Re = u \cdot D/v$, where u is the average inlet velocity, D is the hydraulic diameter and the kinematic viscosity v has been altered so as to make the Reynolds number vary. As foretold by the experimental results in Reference [15], there exists a single re-circulation zone at the expansion corner up to a Reynolds number of about 450, beyond which a second vortex shows up at the top boundary, and gets bigger as the Reynolds number is increased (Figure 3).

The reattachment locations of the vortices are defined as follows; s_1 is the reattachment location of the primary vortex, s_2 is the separation location of the secondary top boundary vortex and s_3 is the reattachment location of the secondary vortex. All of them have been measured from the expansion corner, as depicted in Figure 4.

As seen in Figures 5–7, the computed results obtained in the present work compare more favourably with experimental data than the numerical results from Armaly. Although the

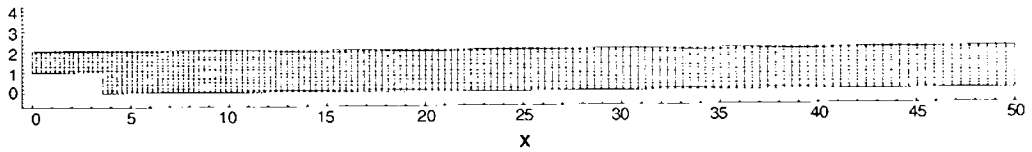

Figure 2. Backward facing step. Mesh.

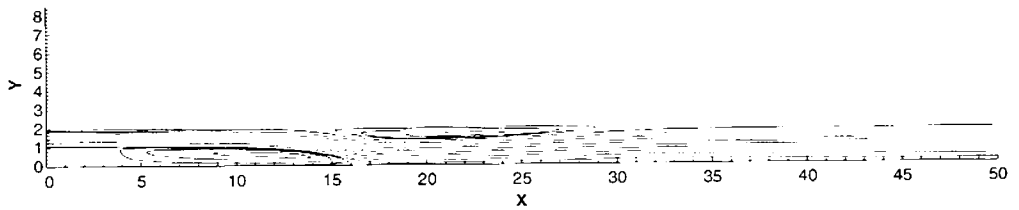

Figure 3. Flow in a backward facing step. Streamlines for Reynolds = 1200.

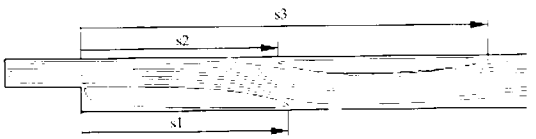

Figure 4. Flow over a backward facing step. Sketch of the recirculation lengths.

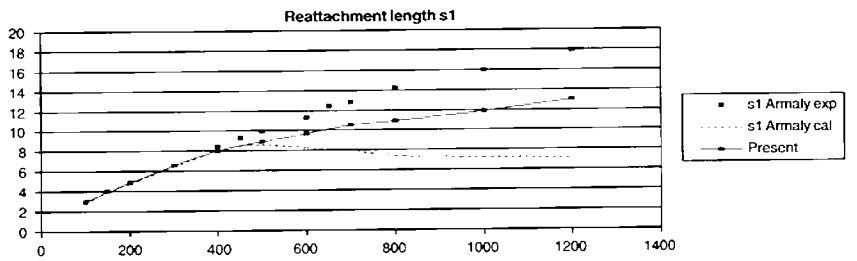

Figure 5. Reattachment length s_1 versus Reynolds number for the backward facing step.

present results are totally analogous to the experimental data in Reference [15] for s_3 and for all the Reynolds numbers considered, when taking about s_2 and specially s_1, the experimental data differ from the calculated results beyond a Reynolds number of about 400. This difference between measured and calculated values is not only shown in the numerical results by Armaly, but also in the results by References [2, 16] among many others. The differences in these values are due to the fact that the 3D effect becomes very important as the Reynolds number is increased. As pointed out by Armaly, these effects became predominant beyond a Reynolds number of 1300.

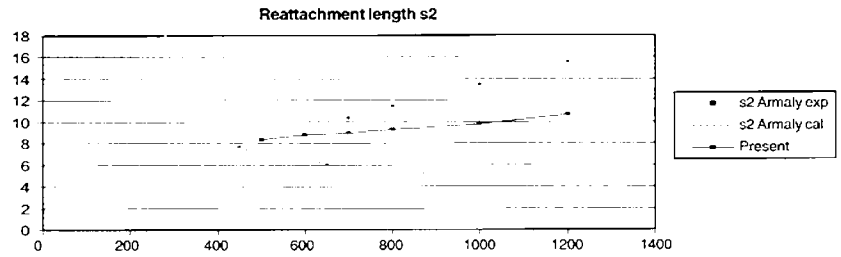

Figure 6. Reattachment length s_2 versus Reynolds number for the backward facing step.

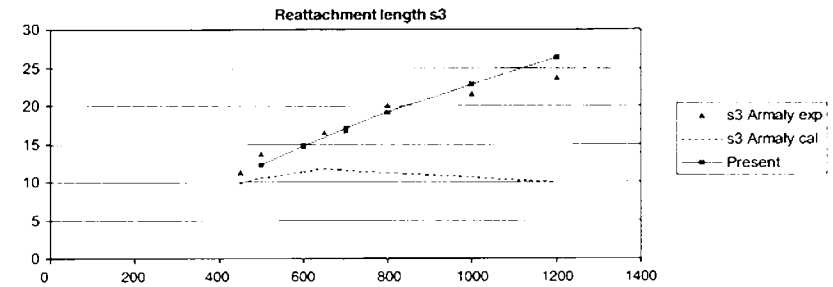

Figure 7. Reattachment length s_3 versus Reynolds number for the backward facing step.

4.2. Application to some wastewater treatment problems

The so defined algorithms create an optimum frame for the evaluation of the flow in some wastewater treatment basins, which is an essential tool in the designing of the wastewater treatment plants for the optimization of their behaviour. Making use of the code, the flow has been evaluated in some conventional wastewater basins of common use, and has also been employed in the design of some newly developed basins for wastewater biological treatment, as part of the research being carried out in the School of Civil Engineering of La Coruña. Some authors have used the potential flow equations to evaluate the flow in clarifiers and other wastewater treatment basins. When we use these simplifications, we can obtain an approximation of the flow for slow creeping conditions, but only the resolution of the all-term-including Navier–Stokes equations will allow us to detect the real streamlines and the vortices that show up even for very slow water flows. Let us now use the previously explained formulations in the resolution of some wastewater treatment basins.

4.3. Flow in a clarification basin

The flow of water in several clarification tanks has been considered. Clarification has two main applications in the water treatment processes. Its most usual aim is to reduce the solids load after coagulation and flocculation have taken place. Its second application is the removal of heavy settleable solids from a turbid source to lessen the solids load in water.

The simplest type of clarification pool is the so-called horizontal-flow sedimentation basin, in either its rectangular, square or circular design. The aim of a good clarification basin design is the obtaining of a sufficiently stable flow, so as to achieve a better sedimentation. There

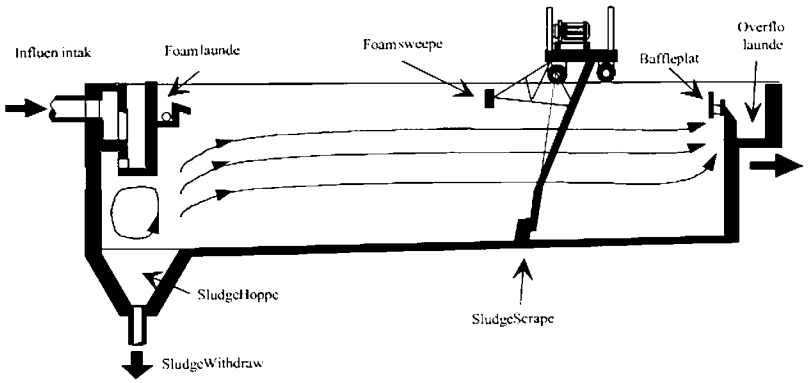

Figure 8. Rectangular clarifier with bottom sludge scraper.

is a large number of non-conventional devices for high rate clarification, such as tube or plate settlers, dissolved air flotation clarifiers, sludge blanket or slurry recirculation clarifiers. The choice of one of those depends on the features of the inflow water, the outflow water requirements, and on the time, space and budget availability to carry out the purification of the water, and should be determined for each particular case. The description of the flow is a powerful tool to attain an optimum shape in the designing of these structures, in order to make the most of the plant resources. The clarification basins calculated as an example have been a rectangular and a circular conventional clarifiers, and also a plate settler. To do so, the laminar penalty Navier–Stokes and the shallow water formulations have been used.

The rectangular and circular basins are the most commonly used clarification devices, in spite of their simplicity, they have achieved excellent results with scant maintenance costs. These basins were originally designed with the capacity to store sludge for several months and were periodically taken out of service for manual cleaning. Today, most of the clarification basins include a continuous cleaning mechanical equipment, such as dragging chains that plow the sludge along the basin floor to hoppers. Nevertheless, these mobile devices for cleaning and other purposes do not have an important influence in the streamline distribution, and can be ignored when the flow is calculated (for further details on clarification basins you can refer to Reference [17]).

4.3.1. Flow in a rectangular clarifier. As a first example, the flow in a conventional horizontal-flow rectangular basin is observed. The tank dimensions are: width 9 m, length 24 m and depth: 3.3 m. A slope of 1.25% has been given to the floor in order to allow for sludge concentration and withdrawal. The design parameters are a detention time 3 h and a surface loading rate of 1 m/h. When working with clarifying basins, one of the criteria to be used in their definition is that of achieving a maximum head loss at the inlet, so as not to disturb the slow flow of the water mass being treated. Therefore, we should avoid turbulence by placing some kind of energy dissipating structure in the faster zone, that is the inlet (see Figure 8). One of these maze-looking dissipating structures has been considered for the inlet of our rectangular clarifier, being placed in the left-hand side. For the outlet, a conventional overflow launder has been disposed in the right-hand side, and the main streamlines are therefore travelling from left to right. For the outlet, a baffle plate has been placed at a

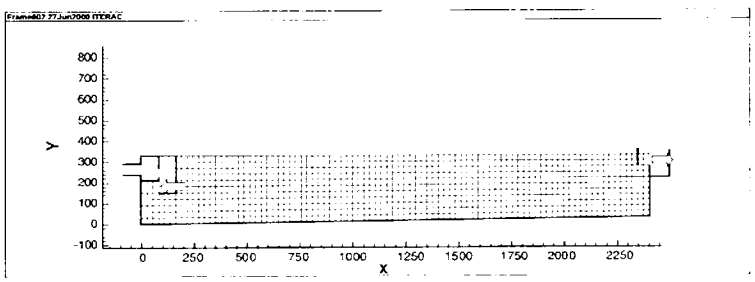

Figure 9. Flow in a rectangular clarifying basin. Mesh.

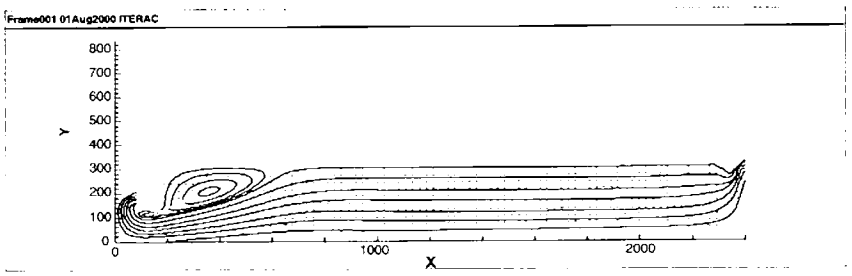

Figure 10. Flow in a rectangular clarifying basin. Streamlines.

distance of 0.5 m from the spillway so as to avoid floating stuff getting into the effluent nozzle.

The domain in which the flow takes place has been split into 949 Q1P0 basic elements with 1052 nodes. For the working parameters chosen and an inflow section of 0.6 m, a velocity of 1 cm/s has been imposed at the inlet. The no-slip condition has been imposed at the bottom and lateral sides, and the spillway has been left free with a zero traction boundary condition. For the topside, the vertical velocity has been fixed as zero and the horizontal velocity has been left free (Figure 9).

As can be seen in the streamline plot (Figure 10), a re-circulation zone happens to occur at the inlet, and a bigger one shows up besides the inflow baffle plate. The first one is a consequence of the leftward direction of the inflow. This is a wanted effect so as not to disturb the flow in the chamber by the entrance of the water. The second and bigger one takes different sizes for varying inflow velocity values, and would vanish for a Stokes analysis that ignores the convective effects. Its existence is an unwanted effect and the basin proportions should be re-designed so as to avoid its existence. Figures 10 and 11 represent the isobars graph and surface plot for the pressure field within a vertical section of the rectangular clarifier, in both of them the pressure is expressed in cm. The so-obtained pressure field is similar to that of the hydrostatic problem as expected.

4.3.2. Flow in a circular clarifier. The other conventional horizontal-flow sedimentation basin considered has been a circular basin with central feeding. The dimensions of the basin are: depth: 3.65 m and diameter: 17.5 m. A slope of 8% has been considered for the bed. The

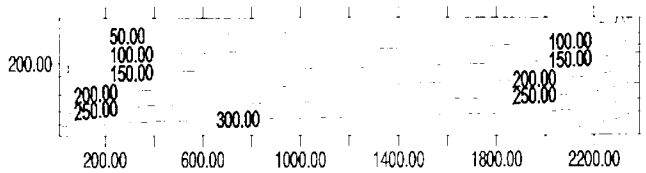

Figure 11. Flow in a circular clarifying basin. Pressures (p/γ) in cm.

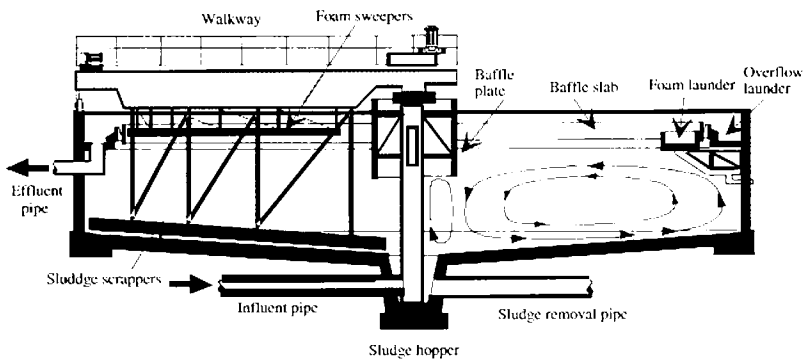

Figure 12. Circular clarifier with bottom sludge scraper. Sketch.

design parameters used in its definition are: detention time 3 h, surface loading rate 1 m/h. To avoid turbulence at the inlet, a 1 m high baffle plate with a diameter of 1.7 m has been placed around the inflow central cylinder, where the horizontal inflow velocity is imposed from height 265 cm up to height 365 cm. The outlets are situated at the circumference perimeter, where an overflow launder endowed with a baffle plate, has been disposed. The flow is obtained by considering a laminar slice that is solved in one half, and then mirrored by the vertical axis so as to obtain the whole flow diagram. Hence, the flow is calculated in a faster way for the same rate of accuracy by using its symmetry property (Figure 12).

This half-domain has been divided into 756 Q1P0 basic elements with 817 nodes. A Dirichlet boundary condition of velocity equal to 1 cm/s has been imposed along the 1 m height of the inlet so as to fit the design parameters. The no-slip condition is again imposed at the bottom and the lateral sides, and the spillway is left free with a zero traction boundary condition. For the topside, the vertical velocity has been fixed as being equal to zero and the horizontal velocity has been left free (Figure 13).

The streamline plot (see Figure 14) shows a primary vortex that takes up most of the room, and two secondary vortices, one of them at the inside bottom zone and a smaller one showing up at the lower external side of the domain. The appearance of these new vortices and the bigger dimensions of the primary one, compared to the rectangular basin, are a consequence of the lesser shallowness of the flow, where the dimension of the vortices depend on the inflow velocity. The pressure values are again similar to those of the hydrostatic problem, and can be seen in Figure 14 in both its isobars plot version, with the pressure units given in cm (Figure 15).

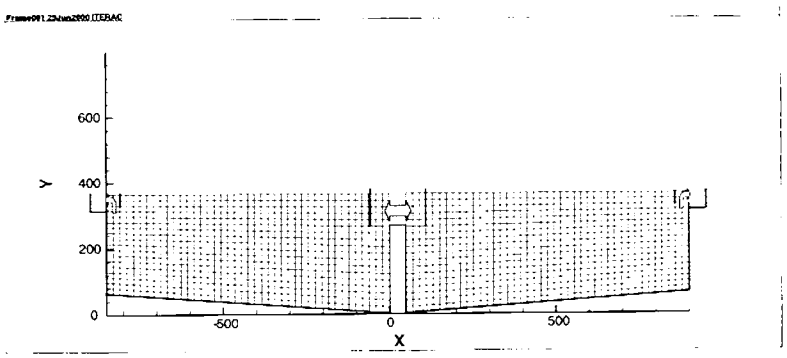

Figure 13. Flow in a circular clarifying basin. Mesh.

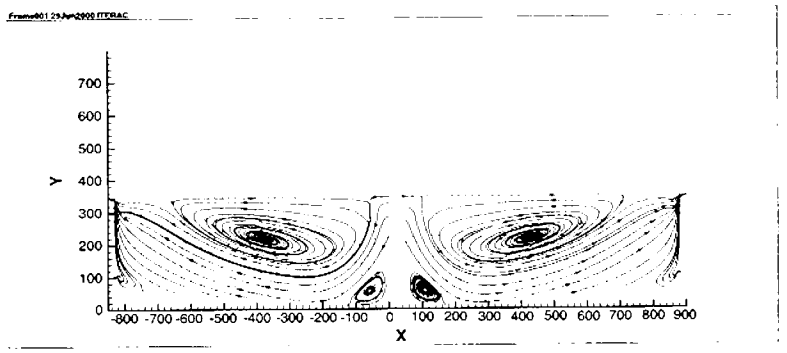

Figure 14. Flow in a circular clarifying basin. Streamlines.

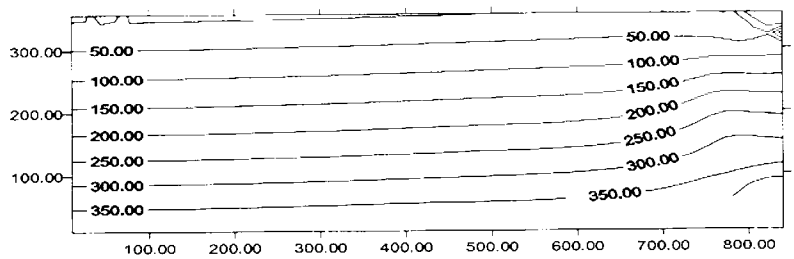

Figure 15. Flow in a circular clarifying basin. Pressures (p/γ) in cm.

4.4. *Flow in a maze flocculator*

The flow along a maze chamber, often used in the flocculation processes, has been calculated. Flocculation is defined as the agglomeration of small particles and colloids to form settleable or filterable particles. A separate flocculation process, where chemical aids are added to water, is very often included in the treatment train to enhance contact of destabilized particles and to build dense floc particles of optimum size. The hydraulic flocculators, in opposition to the

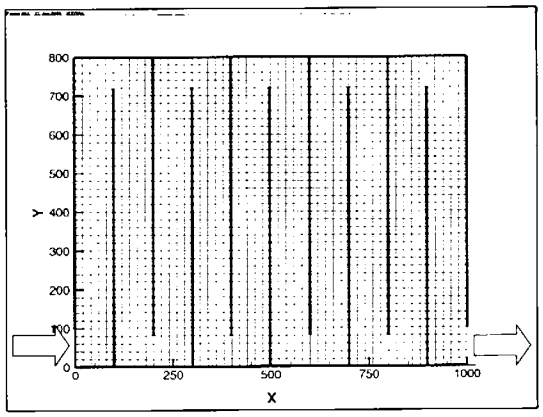

Figure 16. Flow in a maze flocculator. Mesh.

mechanical ones, allow for the formation of the flocs without the help of any mechanical device. This type of flocculation is simple and effective, especially for relatively constant flows. This sort of chambers is also used in chlorination processes. Chlorination forms part of the chemical disinfection treatments that are carried out on supply water in order to achieve its purification and transformation into drinkable water.

The aim of the winding design is to achieve a slow and steady flow over a long distance to allow for the flocs to form. In chlorine disinfection processes, this slowness enables water to maintain contact with the chemical reagent over a long period of time (see Reference [17] for further details on maze flocculators). The velocities involved are quite slow, and a laminar flow is expected, however, small vortices can show up and the Stokes evaluation of the flow could not detect them. For this reason, a convective-term-including formulation is required. A rectangular chamber, in which water is re-circulated along a winding path, often constitutes this kind of basins, and for this particular case will be modelled as a prismatic tank with dimensions 8 m wide and 10 m long, in which a twisting channel is inscribed, split into 10 straight segments. The design parameters chosen for the chlorination tank are the following: tank dimensions $8 \times 10 \times 2\,m^3$, channel width 1 m, channel length 80 m, horizontal velocity 6.6 cm/s, contact time 20.2 min (Figure 16).

A 2091-node regular mesh with 2000 Q1P0 basic elements has been chosen to model the tank. The mixed Shallow Water algorithm has been used with a Manning coefficient of $0.012\,m^{-1/3}/s$. A Dirichlet boundary condition has been prescribed at the inlet, where a parabolic velocity of 6.6 cm/s has been settled at the six lower left-hand-side nodes. At the outlet, the velocity on the six lower right-hand-side nodes has been considered as an unknown, and a hydrostatic pressure boundary condition of 2 m depth has been prescribed. A slope of 10^{-3} has been considered falling rightward all over the domain. A viscosity of $10^{-6}\,m^2/s$ has been used for the wastewater.

As a first guess, the program is used on a Stokes assumption, and the re-circulation obtained is null as expected. The flow is driven 'peacefully' towards the outlet and the parabolic profile is conserved all over the channel length. The results can be seen in Figure 17.

When the convective term is included, small re-circulation zones show up besides the corners. These results are plotted in Figure 18.

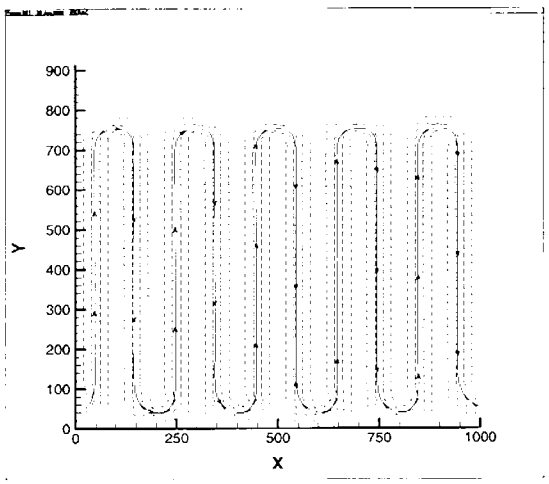

Figure 17. Stokes flow in the maze flocculator. Streamlines.

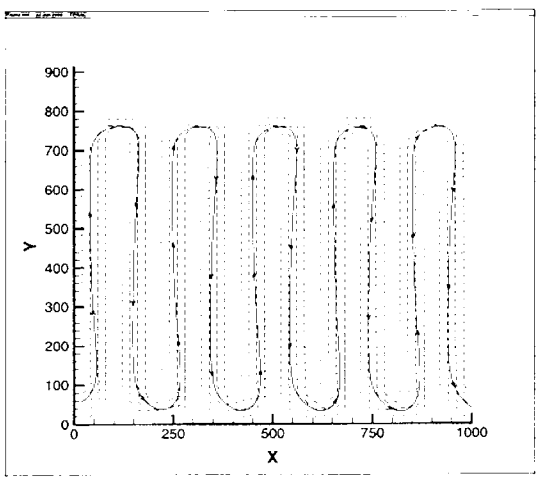

Figure 18. Convective flow in the maze flocculator. Streamlines.

By comparing the results for the Stokes flow and for the full convective-term-including formulation, we can observe some differences in the velocity and streamlines plots. For the first approach the streamlines are kept in an equidistant position with respect to the sides of the winding channel all along the path length, and the parabolic profile of the velocities is also maintained in all the cross sections. Meanwhile, the streamlines in the full convective formulation are sent towards the right-hand side of the channel once they have taken over the corner. The appearance of a small re-circulation area at these twisting zones can also be observed for the convective formulation. This re-circulation is the responsible for both the appearance of sediments besides the corners and also is the cause of a certain energy loss.

These effects are unwanted and could be removed by either carrying out a proper decrease in the velocity of the flow or the re-shaping of the channel.

5. CONCLUSIONS

A stable and computationally efficient code based upon a realistic interpretation of the forces has been written, having proved to provide with optimum results when compared with some reference results. The complexity of the fluid flow creates the need for the use of some numerical devices, so as to avoid the numerical problems that appear in the resolution of the Navier–Stokes equations by the finite element method. One of the sources of instability is that produced by the need of the verification of some consistency conditions. This potential source of instability has been eliminated by an appropriate election in the basic functions and the use of a selective reduced integration for the penalty formulation. As a consequence some spurious solutions, such as the checkerboard pressure modes, have been eliminated and do not appear at all in the present formulation.

The other main source of instability in the obtaining of the flow solutions is due to the presence of the convective term; the symmetric treatment of this term by a standard Galerkin Finite Element formulation is the source of this kind of instability, being the cause of the oscillations that show up in the solution as the Reynolds number is increased. In the algorithms implemented in the code, a stabilization technique of the SUPG type has been used so as to avoid the instability that shows up in the resolution of the pressure and the velocity field when a moderate Reynolds number is used in the calculations. The employment of such a stabilization technique allows us to avoid an excessive refinement of the mesh, in order to prevent the obtaining of the unwanted 'wiggles' in the solution. A SUPG-type stabilization technique that affects all the terms included in the dynamic equation has been used with optimum results providing very accurate and computationally effective results as has been demonstrated in the numerical examples provided.

As a result of the comparison carried out between the present and the reference results, the conclusion is that the solutions obtained by our code compare very favourably with the reference numerical and empirical results by other authors, contributing to a better and faster approach to these problems.

The resolution of the Shallow Water equations is carried out thanks to a newly developed algorithm, which makes use of the finite difference tools within the finite element frame. The evaluation of the friction slope in the Shallow Water equations is based upon on a Manning type formula, which makes use of the empirically determined Manning roughness coefficient. This term accounts not only for the energy losses that take place because of the friction with the wetted perimeter, but also for the overall turbulent losses that take place over the whole domain of integration.

The algorithms regarded in this work provide a perfect frame for the resolution of the flow in some wastewater treatment basins. The evaluation of the pressure and velocity of the flow in these basins provides with useful information about the flow properties that overcomes that found in other related literature. The data about the streamlines and velocity field distribution allows us to know where the main recirculation regions are taking place. This information will be priceless for the purpose of obtaining the geometrical parameters of the basins in order to achieve a better performance for the treatment plant. The obtaining of this optimum

geometry will allow for a further recirculation, if the energy losses are required; or will enable its avoidance if unwanted, modifying in this way the detention times within the basin. The velocity and pressure fields also provide invaluable information about the distribution of the discharge among the outlets, which again can be redefined in order to improve the behaviour of the plant. Thanks to the information obtained by this numerical evaluation of the flow, the water treatment basins and channels can consequently be designed to fit the requirements of the processes being carried out.

ACKNOWLEDGEMENTS

The authors want to express their gratitude to the Environmental Engineering Area of the Civil Engineering School of La Coruña (*Área de Ingeniería Sanitaria y Ambiental de la ETS de Ingenieros de Caminos, Canales y Puertos de La Coruña*), led by Dr Joaquín Suárez. This work has also been partially funded by the European Union FEDER project '*Optimización de circuitos hidrodinámicos y de los procesos en instalaciones de tratamiento físico-químico de agua. Aplicación a la planta de efluentes químicos de As Pontes (1FD1997-0053/HID1,XI/98-X/01)*', the Foundation of Civil Engineering of Galicia (*Fundación de la Ingeniería Civil de Galicia*), the Ministry of Science and Technology (*Ministerio de Ciencia y Tecnología*), the Regional Government of Galicia (Secretaría Xeral de I+D de la Xunta de Galicia) and the private company ENDESA.

REFERENCES

1. Zienkiewicz OC, Taylor RL. *The Finite Element Method*. McGraw-Hill: New York, 1989.
2. Kim SW. A fine grid finite element computation of two-dimensional high Reynolds numbers flows. *Computers and Fluids* 1988; **16**(4):429–444.
3. Choi HG, Yoo JY. Streamline upwind scheme for the segregated formulation of the Navier–Stokes equation. *Numerical Heat Transfer* 1994; **25**(Part B):145–161.
4. Chacón T, Domínguez A. A unified analysis of mixed and stabilized finite element solutions of Navier–Stokes equations. *Computer Methods in Applied Mechanics and Engineering* 2000; **182**:301–331.
5. Hughes TJR, Liu WK, Brooks A. Review of finite element analysis of incompressible viscous flow by the penalty function formulation. *Journal of Computational Physics* 1979; **30**:1–60.
6. Sohn JL, Heinrich JC. A Poisson equation formulation for pressure calculations in penalty finite element models for viscous incompressible flows. *International Journal for Numerical Methods in Engineering* 1990; **30**: 349–361.
7. Hannani SK, Stanislas M, Dupont P. Incompressible Navier–Stokes computations with SUPG and GLS formulations—a comparison study. *Computer Methods in Applied Mechanics and Engineering* 1995; **124**: 153–170.
8. Gartling DK. Finite element analysis of viscous incompressible flow. *Ph.D. Dissertation*. University of Texas at Austin, Austin, 1974.
9. Carey G, Oden J. *Finite Elements*. Prentice-Hall: Englewood Cliffs, NJ, 1984.
10. Sheu TWH, Fang CC. High resolution finite-element analysis of shallow water equations in two dimensions. *Computer Methods in Applied Mechanics and Engineering* 2001; **190**(20–21):2581–2601.
11. Taylor C, Hood P. A numerical solution of the Navier–Stokes equation using FEM technique. *Computers and Fluids* 1973; **1**:73–100.
12. Vellando P. On the resolution of the Navier–Stokes equations by the finite element method using a SUPG stabilization technique. Application to some wastewater treatment problems. *Doctoral Thesis*, Universidad de La Coruña (Spain), Marzo, 2001.
13. Brooks AN, Hughes JR. Streamline Upwind/Petrov–Galerkin formulations for convection dominated flows with particular emphasis on the incompressible Navier–Stokes equations. *Computer Methods in Applied Mechanics and Engineering* 1982; **32**:199–259.
14. Franca LP, Russo A. Recovering SUPG using Petrov–Galerkin formulations enriched with adjoint residual-free bubbles. *Computer Methods in Applied Mechanics and Engineering* 2000; **182**(3–4):333–339.
15. Armaly BF, Durst F, Pereira JCF, Schönung B. Experimental and theoretical investigation of backward-facing step flow. *Journal of Fluid Mechanics* 1983; **127**:473–496.

16. Kwak D, Chang JLC. A three dimensional incompressible Navier–Stokes flow solver. Part I.—INS3D Code. *CFD Workshop*, University of Tennessee Space Institute, Tullahoma, TN, 1985.
17. Metcalf & Eddy INC. *Ingeniería de aguas residuales, tratamiento, vertido y reutilización*. McGraw-Hill: New York, 1995.
18. Choi HG, Choi H, Yoo JY. A fractional four-step finite element formulation of the unsteady incompressible Navier–Stokes equations using SUPG and linear equal-order element methods. *Computer Methods in Applied Mechanics and Engineering* 1997; **143**:333–348.
19. Franca LP, Frey SL. Stabilized finite element methods: II The incompressible Navier–Stokes equations. *Computer Methods in Applied Mechanics and Engineering* 1992; **99**:209–233.